Lab on a Chip

Accepted Manuscript

ROYAL SOCIETY OF CHEMISTRY

www.rsc.org/loc

Lab on a chip for multiplexed immunoassays to detect bladder cancer using multifunctional dielectrophoretic manipulations

Cheng-Hsin Chuang[1]*, Ting-Fe Wu[2], Cheng-Ho Chen[3], Kai-Chieh Chang[1], Jing-Wei Ju[1], Yao-Wei Huang[1], Vo Van Nhan[1]

[1]Department of Mechanical Engineering, Southern Taiwan University of Science and Technology, Tainan 71005, Taiwan

[2]Department of Biotech., Southern Taiwan University of Science and Technology, Tainan 71005, Taiwan

[3]Department of Chem. & Mater. Eng., Southern Taiwan University of Science and Technology, Tainan 71005, Taiwan

*Corresponding author: chchuang@mail.stust.edu.tw

A multiplexed immunosensor has been developed for the detection of specific biomarkers Galectin-1 (Gal-1) and Lactate Dehydrogenase B (LDH-B) present in different grades of bladder cancer cell lysates. In order to immobilize nanoprobes with different antibodies on a single chip we employed three-step programmable dielectrophoretic manipulations for focusing, guiding and trapping to enhance the fluorescent response and reduce the interference between the two antibody arrays. The chip consisted of a patterned indium tin oxide (ITO) electrode for sensing and a middle fish bone shaped gold electrode for focusing and guiding. Using ITO electrodes for the sensing area can effectively eliminate the background noise of fluorescence response as compared to metal electrodes. It was also observed that the three step manipulation increased fluorescence response after immunosensing by about 4.6 times as compared to utilizing DEP for just trapping the nanoprobes. Two different-grade bladder cancer cell lysates (grade I: RT4 and grade III: T24) were individually analyzed for detecting the protein expression levels of Gal-1 and LDH-B. The fluorescence intensity observed for Gal-1 is higher than that of LDH-B in the T24 cell lysate; however the response observed in RT4 is higher for LDH-B as compared to Gal-1. Thus we can effectively identify the different grades of bladder cancer cells. In addition, the

platform for DEP manipulation developed in this study can enable real time detection of multiple analytes on a single chip and provide more practical benefits for clinical diagnosis.

1. Introduction

Bladder cancer is the most malignant tumor affecting the urinary tract and remains a major cause of death worldwide. Patients that are diagnosed with superficial bladder cancer have frequent recurrences of the cancer throughout their lives with threat of progressing to an aggressive advanced stage. Effective detection of bladder cancer biomarkers in immunoassay aims to replace and reduce the use of cystoscopy as a non-invasive technique for diagnosis and surveillance of bladder cancer. Immunosensors are based on the detection of antibody-antigen interactions and can be categorized as utilizing either direct methods where the immuno-chemical complex formation results in physio-chemical changes at the transducer interface or indirect methods based on specific labels attached to one of the immunochemical reaction partners[1]. Immunology exhibits high sensitivity and specificity due to the binding nature of a particular antibody with its corresponding antigen. Nanoparticles (NPs) can be surface modified to improve their ability to bind with antibodies, antigens, enzymes and protein receptors and have been used to enhance detection sensitivity. Examples of use of nanoparticles in biosensing include an impedance sensor for bacteria detection based on bio-functional magnetic beads conjugated with antibodies[2] and the employment of surface modified gold nanoparticles for detecting cancer biomarkers[3-5]. Although nanoparticles have been utilized as probes for immunosensing owing to their attractive properties like high surface area for catalytic activity and adequate size for attaching functional molecules, manipulating them to their predetermined position in an array is still being researched for integration with microfluidic devices. An externally positioned magnet is a common driving force (magneto-phoretic systems) for the rapid collection of magnetic nanoparticles at the target area[6-8]. However this magnetic driving mechanism is limited to magnetic particles and

can possess a challenge when used to guide small concentrations of particles.

Dielectrophoresis (DEP) has been used as an effective and versatile technique for trapping and sorting a wide variety of suspended materials ranging from carbon nanotubes to biological samples of bacteria, cells and DNA[9-12]. DEP is defined as the time-averaged force acting on a spherical dielectric particle immersed in a medium and exposed to a spatially non-uniform electric field[13,14]. The magnitude and direction of this force is dependent on the electric field intensity, particle size and permittivity and also on the conductivity of the particle and the suspension medium. The DEP force can be generated either by a non-uniform AC electric field or a DC electric field due to the induced dipole on the particle surface. However, a DC bias usually has hydrolysis issues and bubbles can occur at the electrode surface where we want to immobilize the nanoprobes (bio-recognition element employing nanoparticles conjugated with antibodies). Hence, we employed AC signals to generate a positive DEP force for trapping and immobilization of nanoprobes on the electrode surface. The feasibility of nanoparticle manipulations by DEP has been demonstrated for different kinds of sensors including thermal sensors[15], humidity sensors[16] and immunosensors[17,18]. Most studies employed electrodes made of opaque metals like gold (Au), platinum (Pt) and copper (Cu). In our previous work[19,20] we had observed that the Au electrodes in the immunosensor chip could induce background noise in the fluorescence response, which reduced the sensitivity of immunosensing. In addition electrodes have also been used for concentrating and guiding to increase the rate of capture[21] and it was observed that the DEP force could resist the effects of Brownian motion and the Stokes force when the particle size was greater than 20nm.

Recent studies have used protein biomarkers for bladder cancer such as Annexin 1[22], Lactate Dehydrogenase B (LDH-B)[23] and Galectin-1 (Gal-1)[24] to verify the relevance of their expression levels to the prognosis of recurrence. Currently the protein expression is usually determined by techniques like immunohistochemistry[25]; western blotting[26] and enzyme-linked

immunosorbent assay (ELISA)[27]. Despite the widespread use of these analysis methods for detection of specific proteins in given samples of tissue homogenate, their procedures require both complex sample preparation and instrumentation. Clinically, fluorescence microscopy has been widely used to detect the fluorescent response which is activated on conjugation with biomarkers and can quickly and accurately reflect their expression levels[28]. In this study, nanoprobes made of alumina nanoparticles bio-modified with antibodies were introduced into the sensing chip and concentrated using a focusing and guiding electrode and immobilized on an SU-8 micro-cavity dot electrode array by DEP force for immunosensing based on fluorescent response. The immunosensor chip employing a combination of electrodes with specific functions as used in our study was easy to control using PC based programming and could effectively transport the nanoprobes to the target area (Fig.1). By performing immunoassay using multiple antibody arrays on a single lab on a chip (LOC), we successfully used cancer cell lysates to detect bladder cancer staging.

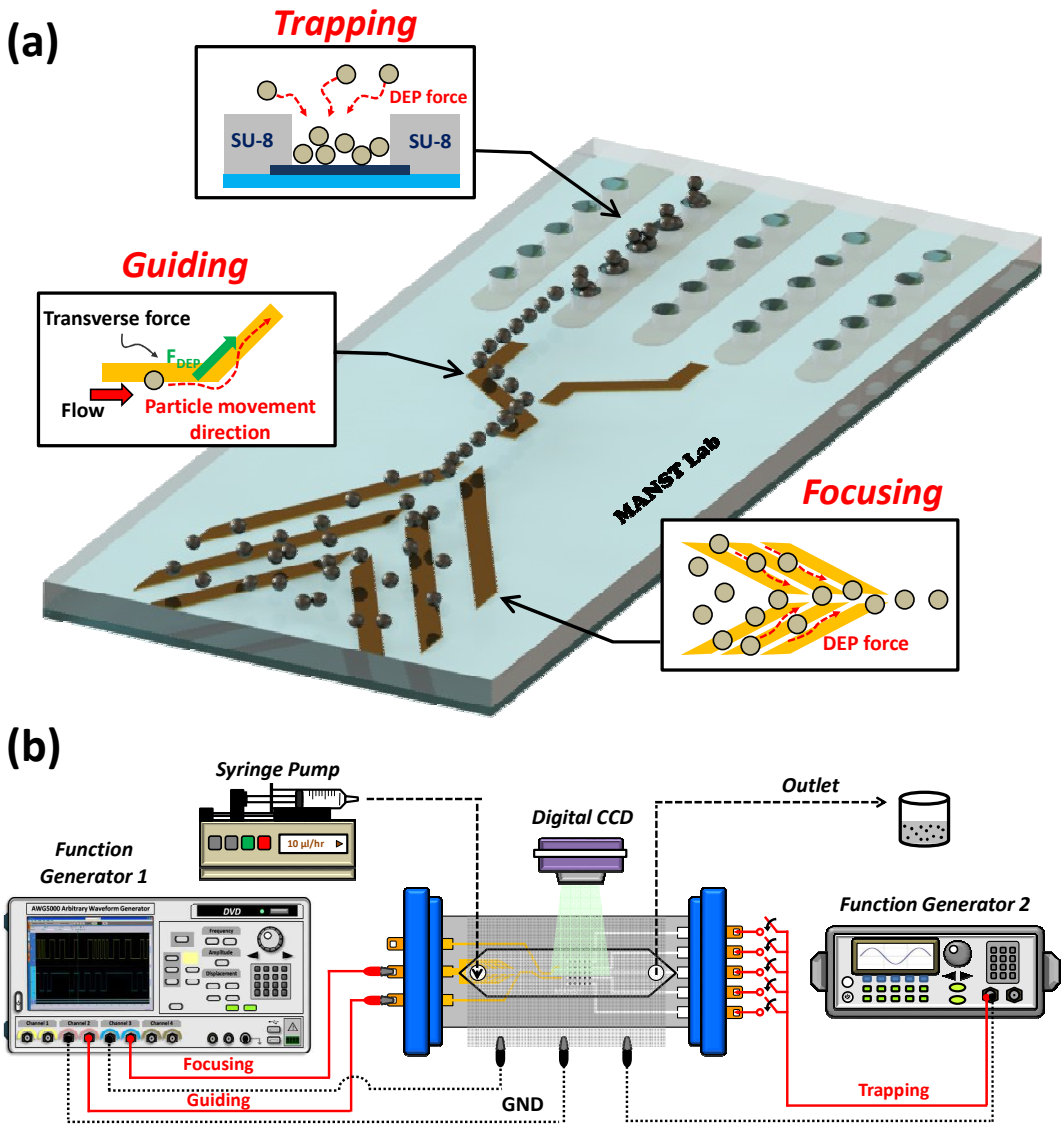

Fig. 1 (a) Schematic diagram of three step DEP manipulations for focusing, guiding and trapping of nanoprobes for improved immunosensing efficiency. (b) Schematic of programmable control of DEP manipulations using function generators and detection of fluorescent response using digital CCD camera mounted on a microscope.

2. Experimental

2.1 Preparation of nanoprobes

The nanoprobes were prepared using a multi-step process that first involves modification of alumina nanoparticles (Al_2O_3-NPs) with silane followed by conjugation with antibodies (Fig.2). Commercially available alumina nanoparticles (Al_2O_3-NPs) with an average diameter

of 50nm were purchased from Evonik Degussa Taiwan Ltd. (AEROXIDE® Alu C, Evonik Degussa). The surfaces of Al_2O_3-NPs were modified with amino groups (-NH_2) by using a silane solution (3-aminopropyltrimethoxysilane, MERCK). In a typical process, 3g of ethanol with a 95% concentration, 1.5 g DI water (Millipore Direct-Q® 3 system) and 1.25g of silane solution were mixed and stirred at room temperature for 3 hrs. Then 2.7 g Al_2O_3-NPs and 100g of 95wt% ethanol were mixed by a Homo Mixer (HM-302, HSIANGTAI) for 10 min. The two solutions were mixed and stirred at 70°C for 3 hrs. Next, the suspended nanoparticles were precipitated by centrifuging (CN-2200, HSIANGTAI) three times at 4000 rpm for 10 min. The sedimentary nanoparticles were pipetted out and baked at 60°C for 12 hrs and it was observed that the silane modified Al_2O_3-NPs were slightly larger than the unmodified Al_2O_3-NPs. In this study, we used two specific antibodies, namely galectin-1 (Gal-1) and Lactate Dehydrogenase B (LDH-B) as biomarkers for the detection of different grades of bladder cancer cell lysates. Before conjugation, the two antibodies were first oxidized in a solution containing 1 mM of sodium metaperiodate and 0.1 M sodium acetate with the solution pH maintained at 5.5. The oxidized antibody was then mixed with Al_2O_3 NPs under constant stirring at room temperature for 30 min. During the oxidizing reaction, the hydroxyl groups (-OH) in carbohydrate moieties of the antibodies were oxidized to aldehyde groups (-CHO), which then subsequently reacted with the amino groups (NH_2) exposed on the surface of Al_2O_3 NPs. This allows the fragment crystallizable (Fc) region or the tail region of the antibody to be attached to the Al_2O_3 NPs while the fragment antigen binding (Fab) region is available for binding during immunoassay. Following the conjugation reaction, antibody-modified Al_2O_3 NPs were collected by centrifugation at 18,000 × g for 5 min. These nanoprobes are referred to as Gal-1/Al_2O_3 and LDH-B/Al_2O_3.

2.2 Preparation of bladder cancer cell lysate

The human urinary bladder urothelial carcinoma cells (T24 and RT4) were purchased from the Bioresource Collection and Research Center, Hsinchu, Taiwan and cultured at 37°C in

McCoy's 5A medium [GIBCO (Life Technologies Corporation), Grand Island, N.Y., U.S.A.] supplemented with 10% fetal bovine serum. The T24 and RT4 cell lysates were harvested and lysed using a mammalian protein extraction buffer (GE Healthcare) according to the manufacturer's suggestions. The protein concentration was determined using the Bio-Rad DC protein assay kit. The original concentration of T24 and RT4 cell lysate was 1μM which were collected from the T75 flask with～90% cell confluency. For fluorescent detection, the cell lysates are labeled using a red fluorescent Cyanine (Cy3) dye purchased in powder form from GE Healthcare (PA23001). The Cy3 powder was mixed with 0.1M sodium carbonate (Na_2CO_3) solution (pH=9.3) and 200ug of T24 protein was added to 100ul of dye solution. After being left for 30 min at room temperature, the labeled T24 proteins were ready for immunoassay.

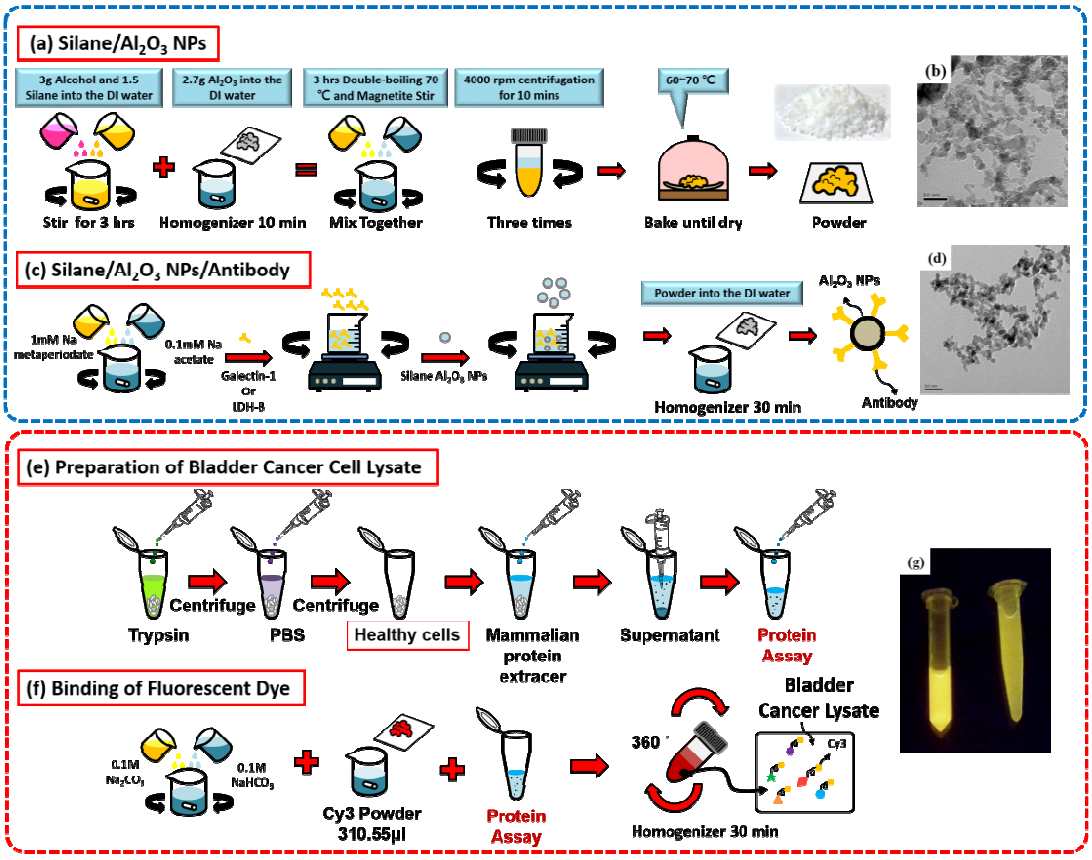

Fig. 2 Sample preparation of nanoprobes and cancer cell lysates. (a) Modification of alumina nanoparticles with amino (NH_2) groups using 3-aminopropyltrimethoxysilane. (b) BF-TEM image of surface modified alumina nanoparticles. (c) Conjugation of modified alumina nanoparticles with antibodies (biomarkers Gal-1 and LDH-B) to synthesize the nanoprobes. (d) BF-TEM image of

prepared nanoprobes that will be immobilized on immunosensor device for detection of different grade bladder cancer cell lysate. (e) Harvesting T24 and RT4 cell lysates using a mammalian protein extraction buffer. (f) Binding of cell lysates with cyanine dye for observing fluorescence response during immunoassay.

2.3 Fabrication of the LOC immunosensor

The LOC immunosensor had two electrode layers, namely gold for the middle electrode and ITO for the bottom sensing electrode. The five part fabrication process of the multi-antibody array based LOC has been illustrated in Fig.3. The five bottom line electrodes with a line width of 40μm for trapping nanoprobes were patterned by standard photolithography and wet etching on 25 × 60 mm^2 ITO glass. Next, an SU-8 micro-cavity array was patterned with a dot-array photomask. The diameter, spacing and depth of the micro-cavity array were designed as 20 μm, 100 μm and 10 μm, respectively. A total of 5 by 5 microcavities were fabricated on five bottom line electrodes. The chip was then cleaned in DI water and dried with a nitrogen gun. Then, 300 Å of chromium and 700 Å of gold were evaporated sequentially onto the chip surface by an E-beam evaporator under temperature control. A photolithography process was then used to pattern the middle electrodes into a fish-bone structure with a width of 30 μm. Previous results of experiments and simulations have shown that an optimal guiding ratio (>90%) could be achieved at a small expanding angle of the guiding electrode (15°) with a low flow rate (0.1ml/hr)[22]. A rectangular flow chamber with dimensions W × L × H = 4 mm × 30 mm × 50 μm was then formed by an optically clear adhesive (OCA) tape attached to the ITO glass. Finally a drill was used to make the holes on the the ITO glass for installation of inlet/outlet tubing. Thus a vertical non-uniform electric field was generated in the flow chamber with the middle electrodes providing the focusing and guiding of the suspended nanoprobes and the bottom electrodes providing effective immediate trapping into the SU-8 microcavities. Consequently, a low-cost, transparent, disposable multiplexed immunosensor was fabricated.

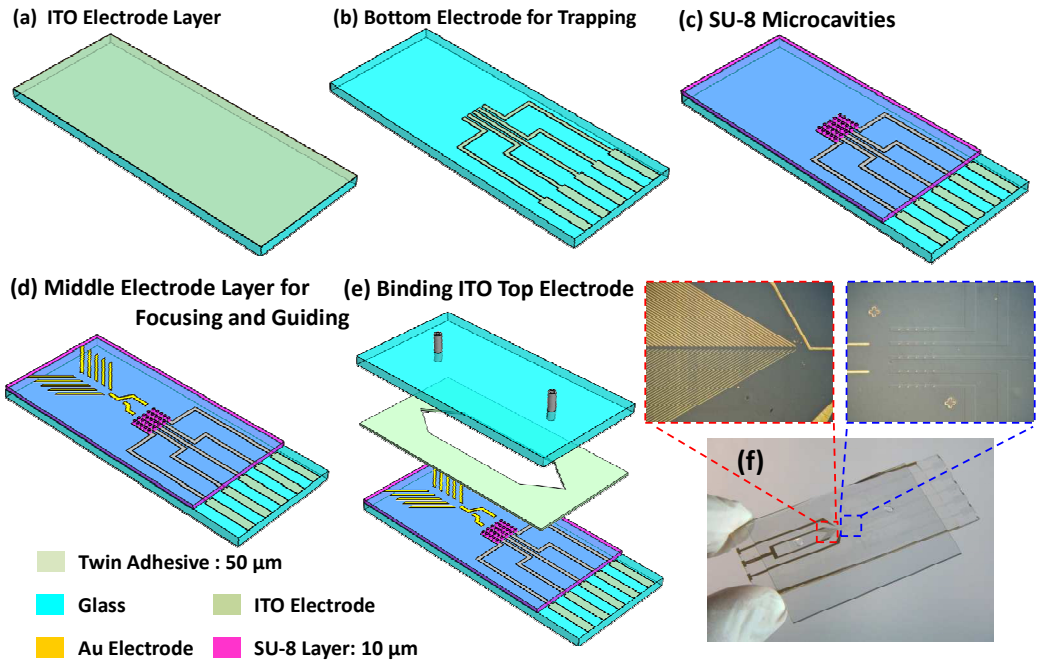

Fig. 3 (a-e) Schematic of step by step fabrication for multiplexed immunosensing on a single LOC. (f) Image of completed device with enlarged images of patterned middle gold electrodes and bottom ITO electrodes as observed under an optical microscope.

2.4 Working mechanism of LOC immunosensor

A syringe pump (KDS-100, KD Scientific) was used to control the flow rate of suspension, and an AC signal was generated by a function generator (AFG3022, Tektronix) for DEP trapping of antibody-Al_2O_3 nanoprobes. In order to get consistent DEP results, the conductivity and pH values of the nanoprobes suspension were adjusted by a conductivity meter (SC-170, Suntex, Taiwan) and a pH meter (TS-100, Suntex, Taiwan), respectively (Table 1).

	PH Values	Conductivity (μs/cm)	Focusing Electrode		Guiding Electrode		Trapping Electrode	
			Frequency (kHz)	Voltage (Vpp)	Frequency (kHz)	Voltage (Vpp)	Frequency (kHz)	Voltage (Vpp)
Gal-1 nanoprobe	7.92~8.55	380~552	700~900	10	500~700	7	16~20	10
LDH-B nanoprobe	8.15~8.44	477~617	1,000~1,200	10	700~1,400	7	9~12	10

Table 1: Details of experimental parameters used in the three step DEP manipulations of nanoprobes

The immobilization steps are separately carried out for the two kinds of nanoprobes containing Gal-1 and LDH-B antibodies. The nanoprobes suspension (Gal-1/Al_2O_3) was first pumped into the flow chamber by a syringe pump at a flow rate of 10 ml/h for about 1 min to fill the flow chamber. Then, a continuous slower flow rate of 0.1 ml/h was used for effective trapping of the nanoprobes. Once the flow is stabilized, the nanoprobes were focused onto the electrode surface by a positive DEP force using an applied AC signal (10 V_{PP}) and frequency of 700~900 kHz. Then, the frequency was adjusted at 500~700 kHz to follow along the gold guiding electrodes and trap them into the SU-8 micro-cavity using the bottom ITO electrode. After the trapping process, the AC signal was stopped and a continuous flush of TTBS at 5 ml/h was applied to the flow chamber for 5 min so that the non-immobilized nanoprobes could be purged to the waste reservoir. The second nanoprobes suspension (LDH-B/Al_2O_3) was then immobilized by repeating all the steps and thus we can fabricate a multiplexed immunosensor. The remaining active sites were blocked by using control BSA protein for 30 min. In the final step, the cell lysate of bladder cancer with a fluorescent label was introduced into the chamber to immunoassay for 60 min. A digital CCD (XC10, Olympus) camera was mounted on a biological microscope (BX51, Olympus) for monitoring the DEP force acting on the

nanoprobes and was utilized to capture the fluorescent images for 100 ms at 10 min intervals for 1 hour. The amount of analyte bound correlates to the intensity of the fluorescent signal obtained. The fluorescent intensity was calculated by an image processing software (Quantity One, BIO-RAD, USA). In order to define the fluorescent response, we normalized the variation of fluorescent intensity between 0 min and 60 min by the intensity at 0 min ($\triangle I/I_0$, where $\triangle I = I_{60} - I_0$, and $\triangle I/I_0$ is the enhancement ratio of fluorescent intensity). Thus, the enhancement ratios for immunosensing of different grades of bladder cancer cell lysates using multiple nanoprobe suspensions can be evaluated.

3. Results and Discussion

3.1 Effects of DEP manipulations on immunoreaction response

In order to compare the efficacy of the three step dielectrophoretic manipulations, we performed an immunoassay of the T24 cell lysate on the multi-array LOC using four arrays (A-1, A-2, A-3 and A-4) in which the nanoprobes have been immobilized with and without applying DEP. For array 1 (A-1), we applied a DEP force only on the ITO electrodes to trap the nanoprobes in the SU-8 micro-cavity array without using the gold electrodes for guiding and focusing. For array 2 (A-2), a combination of the middle gold and bottom ITO electrodes was used for focusing, guiding and trapping. Arrays 3 and 4 (A-3, A-4) in this experiment are used as reference without any DEP manipulations in the absence of applied voltage (Fig. 4b). According to the experimental results, the fluorescence intensity observed in A-1 and A-2 continues to increase as immunoassay time increases. However, A-3 and A-4 showed an absence of fluorescence response. This implies that the nanoprobes were conformally immobilized through cluster formation in the microcavities by the DEP force and reached the immunoreaction site quickly. It was observed that more fluorescent proteins could be bound during immunosensing in A-2 as compared to A-1 and this further validates the use of three

step DEP manipulations to achieve increased sensitivity. In addition, the different nanoprobes utilized in the multi-antibody immunosensor do not influence each other in A-1 and A-2 when DEP force is utilized, thus reducing protein cross-contamination.

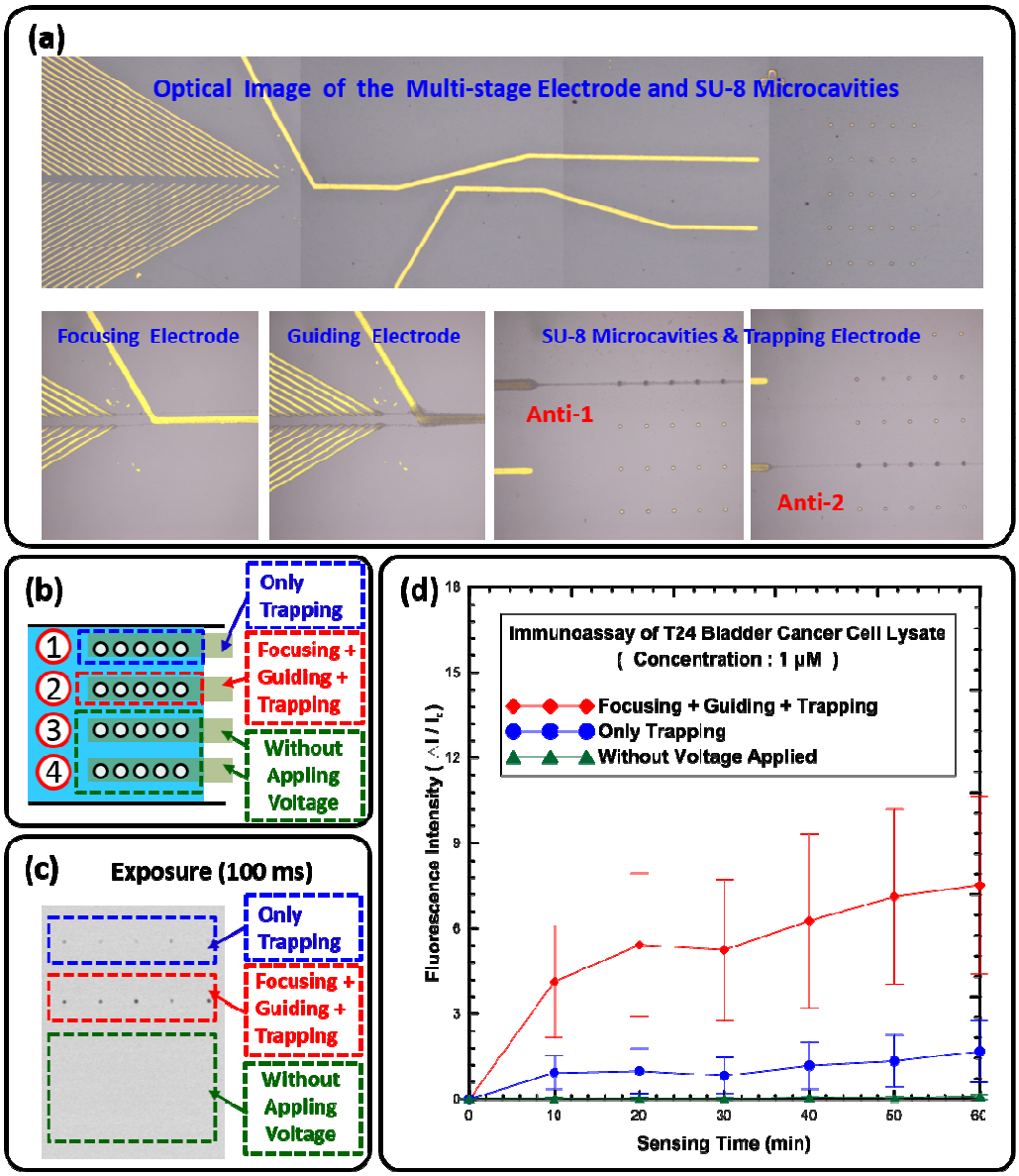

Fig. 4 (a) Optical microscopy images of patterned gold electrodes for focusing and guiding of nanoprobes using patterned gold electrode and SU-8 microcavities for trapping using the bottom ITO electrode. (b) Immunosensing on LOC with and without the use of DEP manipulations. (c) Fluorescence response observed on exposure to different grade bladder cell lysates for 100ms. (d) Enhancement ratio of fluorescence intensity for 1μM T24 lysate after 1 hour immunosensing with/without applying DEP force.

The fluorescence intensity results were recorded immediately after the cell lysate suspension was introduced into the flow chamber and the fluorescence intensity under each immunosensing condition could be plotted against immunosensing time (Fig. 4d). It can be seen from the results that the fluorescence intensities for A-2 (indicated by the solid lines with ◆symbol) and A-1 (indicated by the solid lines with ● symbol) significantly increased after 10 min (the normalized fluorescence intensities are about 4.4 and 0.9 times respectively) and continued to increase. The fluorescence response by using focusing, guiding and trapping (A-2) is about 4.6 times higher than only using trapping (A-1) and tends to stabilize after 40 min. In addition, the fluorescence response obtained using focusing, guiding and trapping (A-2) is about 125 times greater than that obtained without using an AC signal as used in A-3 and A-4 (indicated by the solid lines with ▲ symbol). Thus, we have developed a multifunctional electrode system for efficient DEP manipulations of nanoprobes to significantly improve immunoassay efficiency.

3.2 Comparison of fluorescence intensities for different antibody/cell lysate interactions

We compare the fluorescence intensities for the two kinds of nanoprobes (Gal-1/Al_2O_3 and LDH-B/Al_2O_3) in presence of grade III T24 and grade I RT4 cell lysates in immunoassay. The expression level of Gal-1 antibody in T24 cell lysate is higher than in RT4 cell lysate after an hour of immunosensing with 1.5 times higher fluorescent intensity response as compared to LDH-B; on the other hand, the expression of LDH-B antibody in RT4 cell lysate is higher than in the T24 cell lysate with 1.35 times higher fluorescent intensity response as compared to Gal-1 (Fig 5a). The immunoreaction for different grade bladder cancer cell lysates can thus be effectively distinguished using this method. We conclude from the experimental results that grade III bladder cancer cells will produce a large number of post-cancerous Gal-1 proteins while grade I bladder cancer cells will produce LDH-B proteins. The ability to detect specific proteins (Gal-1 or LDH-B) from a multitude of other proteins present in cell

lysate highlights the selectivity of the immunosensor due to the programmable DEP manipulations. In other words, if a large number of nanoprobes are efficiently guided and trapped in the SU-8 cavities, then amplified signals can be obtained after immunosensing with cell lysate. Our fluorescent intensity observations after immunosensing are in agreement with results obtained using the western blotting analytical technique (Fig 5b) and are also mutually consistent with test results obtained in literature[23,24,28]. Thus, we can successfully distinguish bladder cancer cell staging with quick and sensitive detection results obtained under an hour. Furthermore, this LOC can be used to efficiently trap multiple types of nanoprobes on a single chip and hence can be used to detect specific bioanalytes from complex fluids like cell lysates.

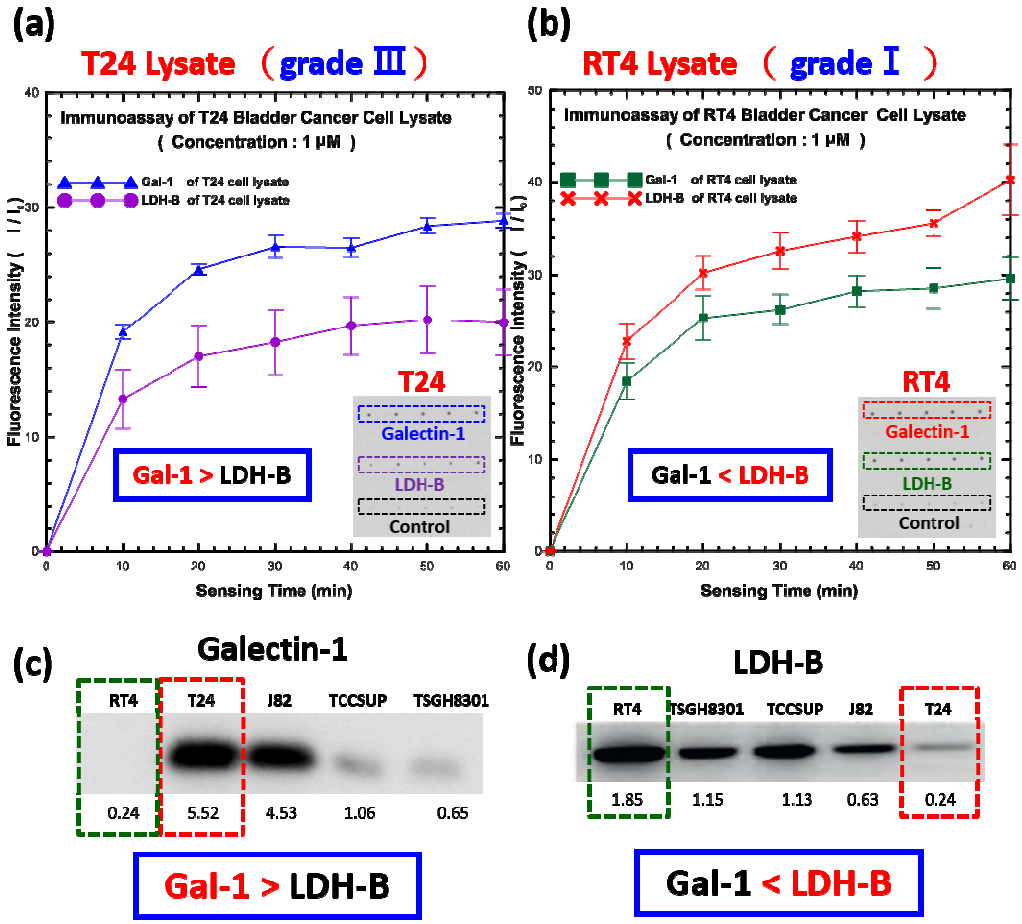

Fig. 5 Fluorescent intensity results for different bladder cancer cell lysates. (a) Gal-1 expression level is higher that LDH-B for grade III T24 cell lysate. (b) LDH-B expression level is higher than Gal-1 for

grade I RT4 cell lysate. (c,d) Verification of immunosensor obtained results with the western blot method.

4. Conclusions

In this study, we successfully developed a LOC device for performing multiplexed immunoassay utilizing novel three step dielectrophoretic manipulations for programmable focusing, guiding and trapping of nanoprobes for significantly improved sensitivity. Experimental results revealed that the immunosensor not only manipulated two kinds of nanoprobes with different antibodies onto the electrode surface, but also achieved detection of different grades of bladder cancer cell lysate and enhanced fluorescence intensity response in immunoassay. Furthermore, the results of fluorescence intensity response for immunoassay of bladder cancer cell lysates corelates with results obtained using the Western Blotting technique. The automated programmable control for multifunctional DEP manipulations can enable the economical scaling up of this LOC device that exhibits high sensitivity, specificity, multiplexing capability and real-time analysis for a wide range of applications. These advantages make it feasible to replace currently used techniques like ELISA and Western Blotting with portable and easy to use LOC devices as fabricated in this study. While DEP manipulations are pivotal in improved immobilization of multiple nanoprobes at the LOC manufacturing end, it is easy to operate in clinical settings and results can be obtained using CCD camera and a microscope. Using this LOC, the bio-recognition element can be further extended from antibodies and antigens as utilized in immunoassays to chemically stable aptamers for DNA/RNA sensing to increase sensitivity and lifetime without a need for low temperature storage, thus enabling economically viable point of care diagnosis.

Acknowledgments

The authors would like to thank the National Science Council of the Republic of China,

Taiwan, for financially supporting this research under Contract No. NSC 102-2221-E-194 -001. Nanotechnology Research Center at the Southern Taiwan University of Science and Technology is appreciated for use of its MEMS fabrication facilities.

References

1 J. Kirch, C. Siltanen, G. Zhou, A. Revzin and A. Simonian, *Chem. Soc. Rev.*, 2013, 42, 8733.

2 X. Yu, H. S. Xia, Z. D. Sun, Y. Lin, K. Wang, J. Yu, H. Tang, D. W. Pang and Z. L. Zhang, *Biosens. Bioelectron.*, 2013, 41, 129-136.

3 K. Y. Chan, W. W. Ye, Y. Zhang, L. D. Xiao, P. H. M. Leung, Y. Li and M. Yang, *Biosens. Bioelectron.*, 2013, 41, 532-537.

4 M. K. Park, J. W. Park and J. H. Oh, *Sens. Actuators, B.*, 2012, 171-172, 323-331.

5 H. Zhang, L. Liu, X. Fu and Z. Zhu, *Biosens. Bioelectron.*, 2013, 42, 23-30.

6 S. Tokonami, M. Iwamoto, K. Hashiba, H. Shiigi and T, Nagaoka, *Solid State Ionics.*, 2006, 177, 2317-2320.

7 S. H. S. Lee, T. A. Hatton and S. A. Khan, *Microfluid Nanofluid.*, 2011, 11, 429-438.

8 L. A. Sasso, I. H. Johnston, M. Zheng, R. K. Gupte, A. Undar and J. D. Zahn, *Microfluid Nanofluid.*, 2012, 13, 603-612.

9 C. Zhang, K. Khoshmanesh, F. J. Tovar-Lopez, A. Mitchell, W. Wlodarski and K. Kalantar-zadeh, *Microfluid. Nanofluid.*, 2009, 7, 633–645.

10 C. L. Asbury, A. H. Diercks and G. van den Engh, *Electrophoresis*, 2002, 23, 2658–2666.

11 K. Khoshmanesh, S. Baratchi, F. Tovar-Lopez, S. Nahavandi, D. Wlodkowic, A. Mitchell and K. Kalantar-zadeh, *Microfluid. Nanofluid.*, 2012, 12, 597–606.

12 R. Zhou, P. Wang, H. C. Chang, *Electrophoresis*, 2006, 1376-85.

13 H. A. Pohl, *J. Appl. Phys.*, 1951, 22, 869–871.

14 H. A. Pohl, Dielectrophoresis: the behavior of neutral matter in nonuniform electric fields Cambridge University Press, Cambridge, 1579 New York. 1978.

15 J. H. Wang, L. Cheng, C. H. Wang, W. S. Ling, S. W. Wang and G. B. Lee, *Biosens. Bioelectron.*, 2013, 41, 484-491.

16 S. L. Leung, M. Li, W. J. Li and J. D. Mai, *Sens. Actuators, A.*, 2012, 178, 32-39.

17 L. Chen and J. Zhang, *Sens. Actuators, A.*, 2012, 178, 88-93.

18 B. Y. Shew, H. C. Chu, C. K. Chen, Y. C. Su, Y. H. Hsieh, L. J. Lai, S. J. Liu and C. H. Leng, *Sens. Actuators, A.*, 2010, 163, 128-137.

19 X. He, C. Hu, Q. Guo, K. Wang, Y. Li and J. Shangguan, *Biosens. Bioelectron.*, 2013, 42, 460-466.

20 C. H. Chuang and Y. W. Huang, *Microelectron. Eng.*, 2012, 97, 317-323.

21 C. H. Chuang, J. W. Ju and Y. W. Huang, *Micro & Nano Letters.*, 2013, 8(10), 659-663.

22 C. H. Chuang and Y. W. Huang, *Electrophoresis.*, 2013, 34, 3111-3118.

23 C. F. Li, K. H. Shen, L. C. Huang, H. Y. Huang, Y. H. Wang and T. F. Wu, *Pathology.*, 2010, 42(1), 43-49.

24 L. C. Liao, C. F. Li, K. H. Shen, L. H. Chien, H. Y. Huang and T. F. Wu, *Pathology.*, 2011, 43(7), 707-712.

25 M. Levin, *J. Biochem. Biophys. Methods*, 58 (2004) 85 – 96.

26 T. Mahmood and P.C. Yang, *N. Am. J. Med. Sci.,* 2012, 429–434.

27 C. M. Cheng, A. W. Martinez, J Gong, C. R. Mace, S. T. Phillips, E. Carrilho, K. A. Mirica and G. M. Whitesides, *Angew. Chem.,* 2010, 122, 4881 –4884.

28 Y. Y. Chan, C. S. Chang, L. H. Chien and T. F. Wu, *J. Ethnopharmacol.*, 2010, 127, 652-661.